Materials Transactions, Vol. 42, No. 2 (2001) pp. 356 to 364

Fracture Morphology and Quenched-in Precipitates Induced Embrittlement in a Zr-base Bulk Glass

Guo He[1,*], Jian Lu[2], Zan Bian[1], Dianjin Chen[2], Guoliang Chen[1], Guochao Tu[2] and Guojun Chen[2]

[1]*State Key Laboratory of Advanced Metals and Materials, University of Science and Technology Beijing, Beijing100083, P. R. China*
[2]*Shougang Metallurgical Research Institute, Beijing 100085, P. R. China*

The fracture morphology and quenched-in embrittlement in $Zr_{52.5}Ni_{14.6}Al_{10}Cu_{17.9}Ti_5$ bulk glass were investigated by tensile and compressive tests at room temperature at the same strain rates of 4×10^{-4} s^{-1} and scanning electron microscopy (SEM) observation. SEM analysis based on the deformation and fracture features indicates that the normal stress and shear stress on the fracture surface play a different role in the shearing-off of the specimens in tension and compression. The shear stress is the main controlling factor for the fracture in compression, and the fracture surface is along the maximum shear stress plane. In tension, however, both the shear and normal stresses govern the fracture process together, and the fracture surface is along the plane with an angle of 56 deg away from the axial direction. The fracture firstly starts from a random region on the surface where there is a stress concentration due to the voids or shear bands. The shearing-off leads to a dilatation and softening of the local glass. The softening then promotes the shearing-off and leads to final catastrophic fracture. The crystalline precipitates significantly influence the tensile and compressive properties. With increases in the volumetric fractions and the sizes of the precipitates, both the tensile and compressive strength and fracture strains decrease. The fracture mode changes from ductile to brittle. Vein patterns, shear-bands and local melting can still be observed when the volume fractions of quenched-in precipitates are less than 3 $\sim$ 5%. When the precipitates exceed 5% in volume fraction, fracture surface becomes rock strata-like feature, and samples lose almost their strength. The precipitates with larger sizes and no-spherical shapes play a role in rising stress concentration, resulting in decreasing the fracture strength.

(Received August 7, 2000; Accepted December 22, 2000)

Keywords: *bulk metallic glass, quenched-in precipitates, fracture, strength, fracture morphology, shear stress*

1. Introduction

Bulk metallic glasses (BMG) have been progressively developed in past decade.[1)] Based on the understanding of their properties, many bulk metallic glasses have potential applications in various areas, such as structural materials using their high yield strength, high hardness, good wear resistance and excellent corrosion resistance. Some BMGs, *e.g.* Fe-based, Co-based and Nd-based, may present good soft magnetism that will lead to the most significant functional applications. Furthermore, some BMGs with both good magnetism and good mechanical properties can be used as a "functional materials with good structural properties, or structural materials with good functional properties".[2)] For example, the good soft magnetism and good wear resistance is useful in tape recorder heads.[3)] On the other hand, the BMGs present superplasticity in the supercooled region. This can be used to fabricate shaped metallic glassy parts. Particularly, the critical cooling rates of Zr-base BMGs for the glass formation are as low as $1–10^2$ K/s. The high glass forming ability makes it possible for the Zr-base BMGs to be used as novel advanced structural materials. However, the ductility of the Zr-base BMGs is very sensitive to the composition and structure. Any devitrification or crystallization may induce embrittlement of the glass for many compositions.[4–7)] This embrittlement certainly leads to dramatically decrease in fracture strength of the BMGs.

Since then, the Zr-base BMGs have been comprehensively characterized in mechanical properties because they can be easily cast into larger diameter (>3 mm) rods or larger thickness sheets (>2 mm).[8)] Though the fracture strength of the BMGs is dependent on their compositions, most of them have higher strength than their counterparts of crystalline alloys. This means that the crystalline in the BMGs would decrease their strength. The fracture strength is closely related to the glass structure and can be manifested from the fracture features. As it is well known, conventional quenched metallic glasses undergo viscous flow deformation at elevated temperatures and low strain rates.[9)] The Zr-base BMGs have a similar deformation behavior with the conventional metallic glass. Under the condition of high temperature and low strain rate, the BMGs exhibits homogeneous flow, by which each volume element of the sample contributes to the strain, so that the test sample presents a superplastic-like deformation behavior. At low temperature, the deformation mode is inhomogeneous flow, and all the plastic flow is concentrated in shear bands, indicating that any flow leads to softening in the localized bands, resulting that the final fracture occurs along the planes of those softening shear bands.[10)] The work softening unfortunately leads to the metallic glassy sample fracture with little plastic elongation in an apparently brittle manner. In the other hand, the fracture mode of Zr-base BMGs is considered as having ductile fracture features,[11,12)] because vein patterns, commonly associated with the fracture of metallic glasses,[13)] and fracture steps can be obviously observed on the fracture surface. Many experiments confirm that the fracture surface and shear-band orientations are about 45° to the sample axis when loading by a compressive stress. This suggests that the shear bands be developed along the plane of maximum shear stresses. When loading by a tensile stress, the orientation of the fracture surfaces and shear-band steps is about 56° to the tensile axis. These orientating behaviors

*Corresponding author. E-mail: he-guo@163.com

in BMGs under applied stress are very similar with that in conventional quenched metallic glasses.

For the crystal/glass composite structure, the crystals embedded in the glass matrix can be classified as two kinds in terms of their forming process and size. One kind already forms during casting due to nucleation in the melt caused by impurities, *e.g.* oxides, or by insufficient cooling rate upon quenching. Such quenched-in intermetallic compounds certainly give rise to a significant brittleness.[7,14,15] An important fact is noted that the as-cast composite microstructures have micrometer-sized crystals in the glassy matrix, which causes significantly reduced ductility even for a small volume fraction of quenched-in crystallites. However, Hays *et al.*[16] reported an exception in Be-containing Zr-base alloys that the ductile β-Ti–Zr–Nb phase primarily crystallizes and dramatically increases the plastic strain and toughness of the metallic glass. These suggest that the μm-size ductile second phase particles distributed in the glassy matrix are beneficial for improving the overall ductility of the metallic glass composite by exhibiting plastic deformation within the ductile particles and by inducing multiple shear band formation.

The other kind of crystallites formed by crystallization of the glass has nanoscale-size, and cause brittleness only for large volume fraction of nanocrystals. For example, Leonhard *et al.*[7] studied the effect of crystalline precipitates on the mechanical behavior of Zr–Al–Cu–Ni and Zr–Ti–Al–Cu–Ni BMGs. They found that the as-cast two-phase microstructures of micrometer-sized crystals in glassy matrix exhibits significantly reduced ductility, but the yield strength remains unchanged compared to the fully glassy material. However, nanocrystalline precipitates produced by annealing of initially fully glass do not decrease the ductility significantly but increase the yield strength if controlling the crystalline volume fraction less than 40%. Larger volume fractions of nanocrystals promote brittle fracture and considerably reduce fracture strength. On the other hand, in some Zr-base BMGs a metastable quasicrystalline phase forms during annealing.[17–20] This phase changes to stable crystalline phases upon annealing at higher temperatures. The available data indicate that the nanosize quasicrystals do not deteriorate the ductility of the Zr-base BMGs.[20] Rather strength increase together with an even slightly improved ductility is found after primary precipitation.

Doglione *et al.*[4] characterized the Be-bearing Zr-base BMG by compressive tests. They compared the fracture toughness of as-quenched partially crystallized and partially nanocrystallized samples. The results indicate that the heat treatment always produces intrinsic embrittlement of the glassy matrix. Furthermore, they conclude that the as-quenched crystalline does not lead to embrittlement. Gilbert *et al.*[5,21] tested the fracture toughness of a similar Be-bearing Zr-base BMG, and revealed that partial and full crystallization by thermal annealing results in a drastic reduction in fracture toughness and loss of ductility. The available investigations indicate that a crack propagates along the interfaces between crystals and glass matrix. The strengthening effect of nanocrystals in the Zr-base BMGs is believed to arise from a strong interaction between the nanocrystals and local shear bands during deformation processes of the glassy matrix.[22] Moreover, retaining a good ductility after partial crystallization is supposed to be related to the nature of the particle/glass interface and the enrichment of certain elements such as Al in the remaining amorphous matrix.[11,12]

Even though some fracture modes of the Zr-base BMGs have been reported in recent years, there are some contradictions in quenched-in precipitates-induced embrittlement in available investigations. The systematic research is certainly required to elucidate the deformation and fracture mechanism in BMGs, especially in the BMGs with quenched-in precipitates. This investigation has a careful observation in detail on the fracture morphology of a Zr-base BMGs with different volume fractions of quenched-in precipitates. The fracture process is directly examined by scanning electron microscopy (SEM). The deformation and fracture mechanism is suggested from the experimental observation and rough thermodynamic calculations.

2. Experimental Procedure

The Zr-base alloy with the nominal composition of $Zr_{52.5}Ni_{14.6}Al_{10}Cu_{17.9}Ti_5$ (at%) was prepared by pre-alloying using electromagnetic levitation under Ar atmosphere, and then re-melting followed by injection casting into cylinders and sheets with various diameters (ranging from 2 to 8 mm) and thickness (ranging from 1 to 4 mm). The fully glassy samples can be obtained when choosing the pure zirconium with oxygen content less than 0.08 mass% and the sample size being less than 3 mm in diameter for cylinders or 2 mm in thickness in sheets. In other hand, two parameters (overheating temperature before casting and sample size) influence the formation of the bulk glass. Small overheating temperature gap, large sample size and high oxygen content would induce the quenched-in precipitates. Their effect on the glass formation have been investigated elsewhere.[23] As-cast cylinders and sheets were sectioned for microstructural analysis. X-ray diffraction pattern (XRD) using Cu Kα radiation, transmission electron microscopy (TEM) and SEM were used to check the glass and quenched-in precipitate microstructures.

The cylindrical samples were used to prepare specimens for compressive tests, and the sheet samples for tensile tests. Compressive specimens were fabricated with 2 mm- to 8 mm-diameters and 3 mm- to 12 mm-length (length : diameter = 1.2 $\sim$ 1.6), the appearance of the compressive specimen is shown in Fig. 1(a). Compressive tests were conducted at room temperature by MTS-810 at strain rates of 4×10^{-4} s^{-1}. The compressive strains were measured from the compressive stress-strain curves or the load-displacement curves. Tensile specimens were fabricated from sheet samples. Their shape and size are shown in Fig. 1(b). Tensile tests were conducted at room temperature by MTS-809 at strain rates of 4×10^{-4} s^{-1}. The tensile strains were measured by the extensometer. Each data of the fracture strength and strain is an average result of more than five tests. The deformation and fracture morphologies of the Zr-base BMGs were extensively investigated by using SEM.

3. Results

3.1 Microstructures and strengths of the Zr-base BMGs

Figure 2(a) is a TEM image of the fully glass morphol-

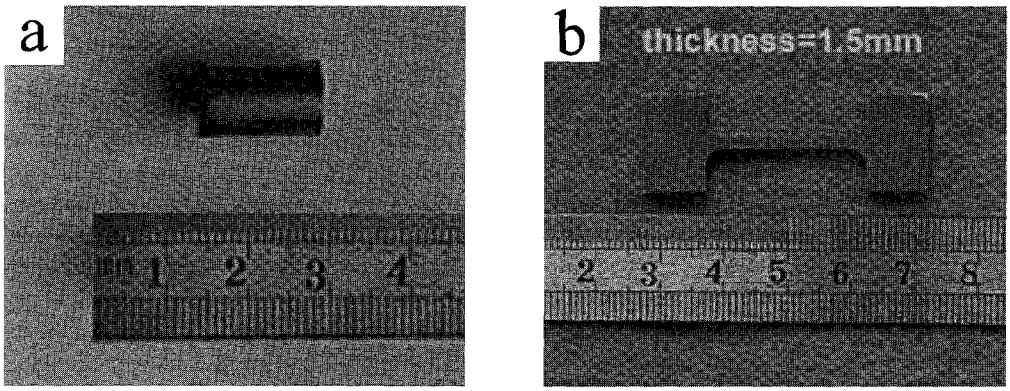

Fig. 1 Appearance of specimens of $Zr_{52.5}Ni_{14.6}Al_{10}Cu_{17.9}Ti_5$ BMG for compressive test (a) and tensile test (b).

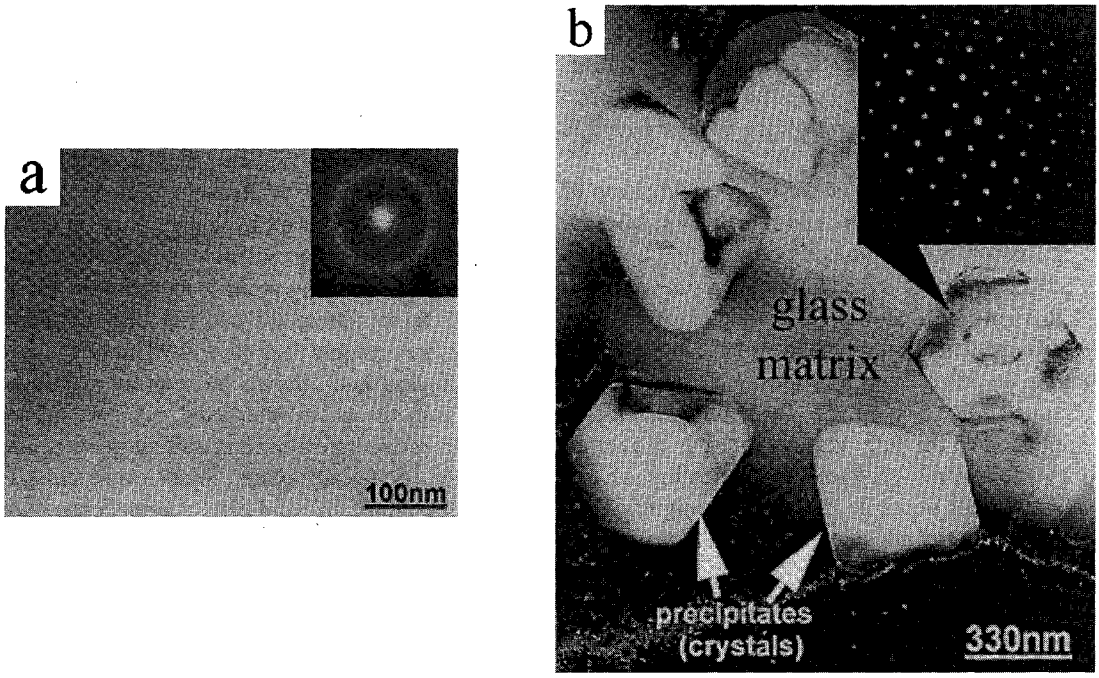

Fig. 2 TEM images and selected-area diffraction patterns of $Zr_{52.5}Ni_{14.6}Al_{10}Cu_{17.9}Ti_5$ BMG samples, (a) fully glass and (b) glass with quenched-in precipitates.

ogy on which a uniform microstructure with no any contrasty phases can be seen. The corresponding selected-area diffraction pattern shows a wide ring. Figure 2(b) is a TEM image of the Zr-base BMG with quenched-in precipitates and the selected-area diffraction pattern on the precipitate. Figure 3 shows the XRD patterns taken from the section of the Zr-base BMG samples, where (a) is for fully glass and (b) is for glass with a volume fraction of crystalline precipitates.

For fully glass, the uniaxial tensile and compressive tests indicate no distinct necking for tension and no significant difference between yield strength and fracture strength for both tension and compression. The fracture strength in uniaxial compression is found to be 1.82 ± 0.13 GPa (14 specimens) and the total strain (including elastic and plastic strains) to be about 1.8%. The fracture strength in uniaxial tension is 1.66 ± 0.42 GPa (5 specimens) and the total strain is about 1.6%. Typical stress-strain curves for the tensile and compressive tests are shown in Fig. 4 (curve 2 and 4). On the tensile curve, very slight plastic deformation without work

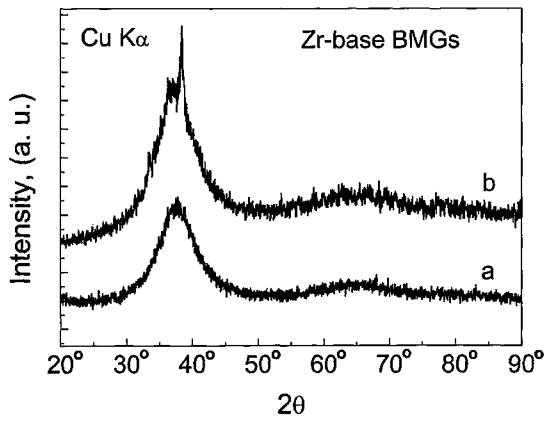

Fig. 3 X-ray diffraction patterns taken from as-cast $Zr_{52.5}Ni_{14.6}Al_{10}Cu_{17.9}Ti_5$ BMG samples, (a) for fully glass and (b) for glass with quenched-in precipitates.

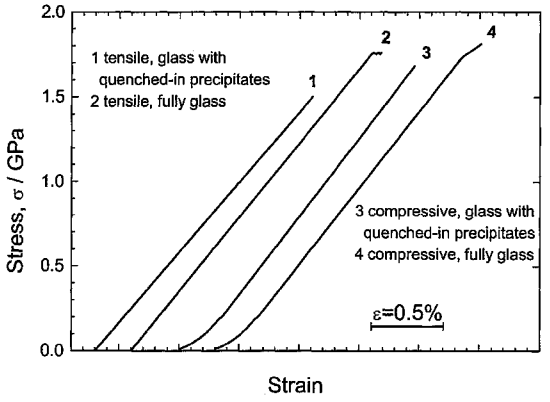

Fig. 4 Typical stress-strain curves of $Zr_{52.5}Ni_{14.6}Al_{10}Cu_{17.9}Ti_5$ BMG for the tensile and compressive tests.

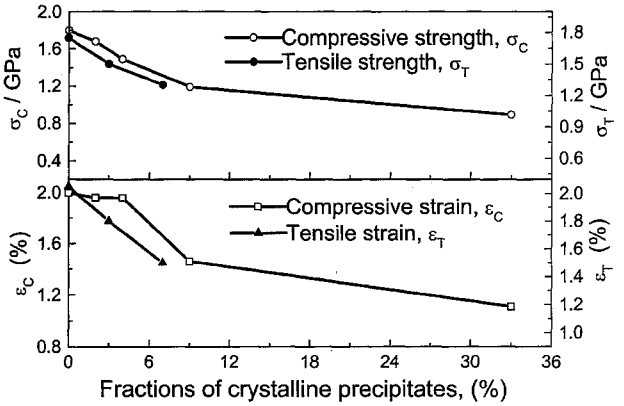

Fig. 5 Effect of the precipitate volume fractions on the tensile and compressive properties of $Zr_{52.5}Ni_{14.6}Al_{10}Cu_{17.9}Ti_5$ BMG.

hardening can be seen. Almost no plastic deformation can be distinguished before fracture on the compressive curve. The features of the stress-strain curves without work hardening and plastic elongations for the Zr-base BMG are very similar with that for other BMGs and conventional quenched metallic glasses. The slight plastic deformation is generated from the accumulation of localized shear bands. The final fracture occurs along the shear band plane.

Figure 4 (curve 1 and 3) shows tensile and compressive stress-strain curves of as-cast $Zr_{52.5}Ni_{14.6}Al_{10}Cu_{17.9}Ti_5$ BMGs with about 3% quenched-in crystalline precipitates at strain rate of 4×10^{-4} s^{-1} respectively. The data reveal a sharp decrease in both tensile and compressive fracture strengths compared with that of fully glass. The appearance of the as-quenched-in crystalline precipitates induces embrittlement of the BMGs, no plasticity is observed on the curves. Further investigation indicates that with increasing the crystalline precipitates, the tensile and compressive fracture strengths decrease quickly, but Young's modulus has no distinct change.

Figure 5 shows the effect of the precipitate fractions on the tensile and compressive properties. It is obviously shown that with increasing the fractions of the crystalline precipitates, the tensile and compressive fracture strengths decrease, and the tensile and compressive fracture strains also decrease. The compressive strengths are reasonably higher than the tensile strengths.

Since the crystalline precipitates with different sizes will affect the deformation behavior by various mechanisms,[24] the maximum sizes of the crystalline precipitates were examined and plotted to tensile and compressive fracture strengths and fracture strains shown in Fig. 6. When the maximum size is around 200 ~ 400 nm, the samples present different sensitive to the maximum precipitates in tensile and compressive properties, indicating different deformative mechanisms for tensile and compressive deformations. With increasing the maximum size of the crystalline precipitates, tensile and compressive fracture strengths decrease, and the tensile and compressive fracture strains also decrease. It should be noted that the precipitates formed in the solidification process are very different from that formed during annealing of the BMGs. The former has a large size about 100 to 500 nm, the later about 10 to 50 nm.[25,26] The precipitates with various sizes would play different roles on strain and fracture modes.

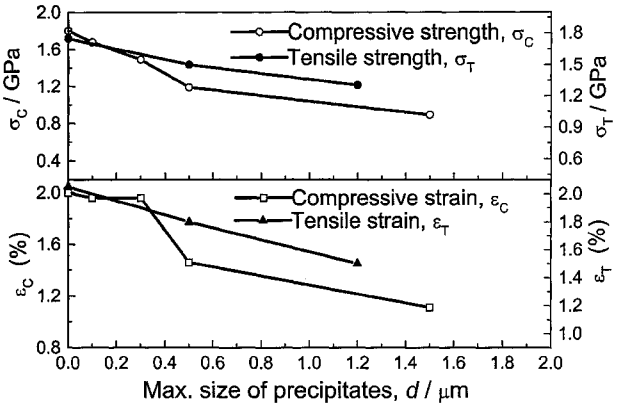

Fig. 6 Effect of the maximum sizes of the crystalline precipitates on the tensile and compressive properties of $Zr_{52.5}Ni_{14.6}Al_{10}Cu_{17.9}Ti_5$ BMG.

3.2 Deformation and fracture phenomenology

For fully glass, although there is no distinct plastic deformation in either tensile stress-strain curve or compressive stress-strain curve, both specimens after fracture have shown obvious and well-distributed shear bands, which are near parallel each other. The shear bands orient by an angle with the load axis which is in the range of 40° ~ 45° for compressive specimens and in the range of 55° ~ 65° for tensile specimens. Figure 7 shows the shear bands on the specimen surface and the fracture surface formed by spitted along the shear bands. The fracture surface just formed near the specimen surface shows initial vein patterns with flow traces towards shear direction shown in Figs. 7(a) and (b). The magnification of the shear bands on the specimen surface shows that the bands have unequal spacing and are not rigorously parallel. Between the shear bands, some voids can be seen from Fig. 7(c), which would be the initiation of cracks under loading, or would speed up the crack propagation by joining the cracks. The average shear band spacing is about 0.2–0.5 μm.

Figure 8 shows a fracture structure caused by partly shearing off along nearly shear band plane under uniaxial compressive loading. From the fracture structure one can find that the shearing-off firstly occurs in several shear bands. Then, the shearing-off proceeds under the loading with the development of the shear bands, and the shearing-off surface extends roughly along the shear band plane. When the process takes

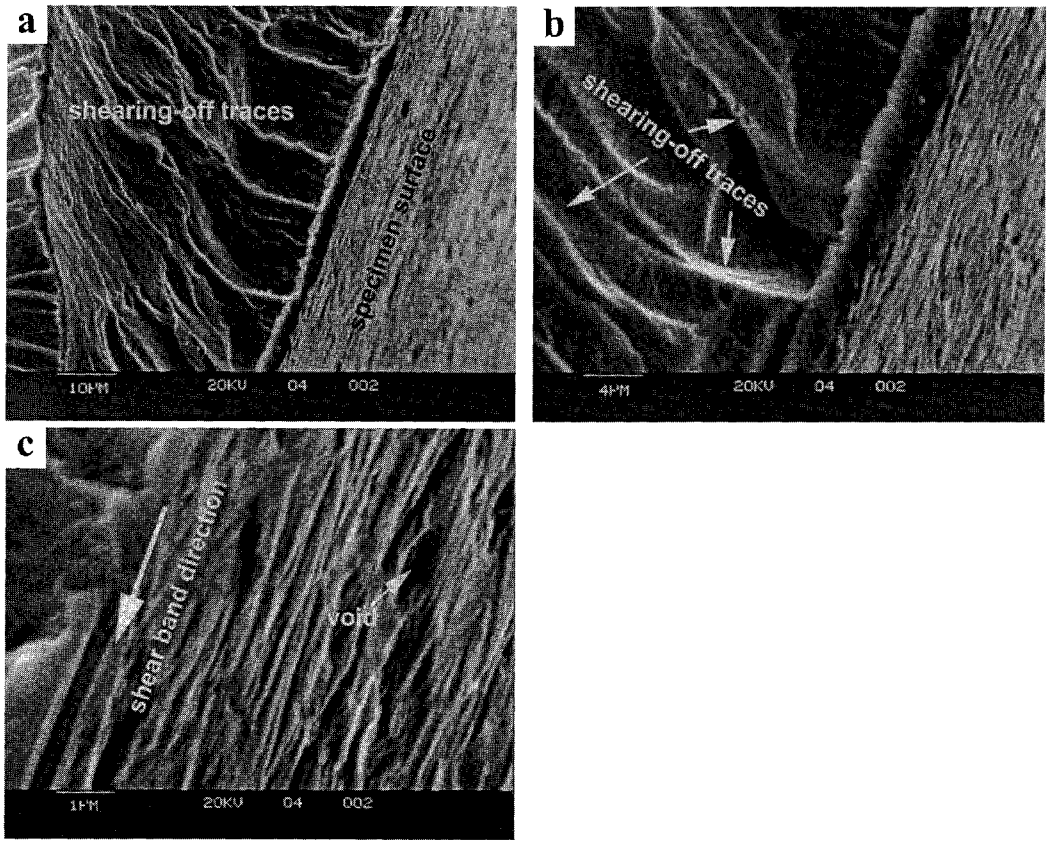

Fig. 7 SEM images of shearing-off traces near the shear bands on the specimen surface (a and b) and the magnification of the shear bands on the specimen surface (c) of $Zr_{52.5}Ni_{14.6}Al_{10}Cu_{17.9}Ti_5$ BMG under compressive loading at room temperature.

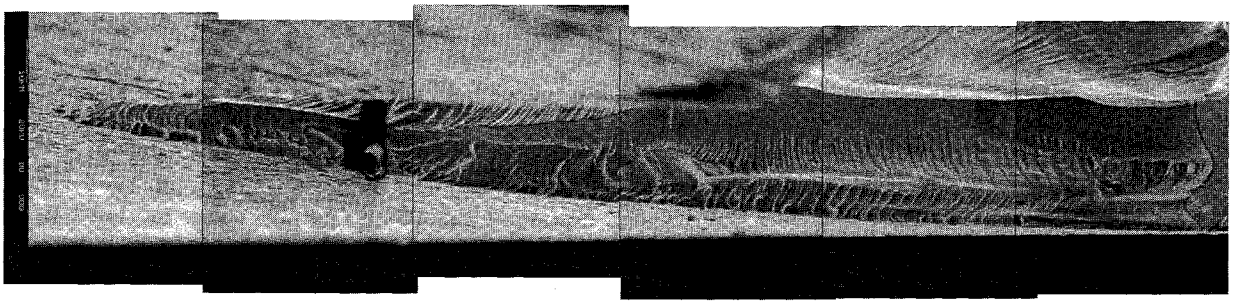

Fig. 8 SEM images of partially shearing-off of a $Zr_{52.5}Ni_{14.6}Al_{10}Cu_{17.9}Ti_5$ BMG specimen under compressive loading at room temperature.

place, the shearing-off surface seems to deviate its orientation to the maximum shear stress direction. This suggests that the maximum shear stress may play an important role in causing the fracture. On the images, it is easy to count the number of the shear bands that participate the fracture flow, which are about 100–200 shear bands. There are about 10–20 shear bands yielding on the tip of the shearing-off crack. With the shearing-off developing, more shear bands yield and joint to flow and form the flowing traces, *i.e.* vein patterns on the fracture surface.

The fracture surfaces for the Zr-base BMG present a typical ductile fracture feature. Figures 9(a) and (b) show the typical fracture surface with vein pattern morphology for fully glass. Most of the fracture surface has such kind of the vein pattern that extends towards the maximum shear stress direction. Figure 9(c) shows the region on the fracture surface where is finally separated when fracture occurs. Some coarse and rough contours of the veins (white color in Fig. 9(c)) are generated that contain large amounts of voids, which leading to the local volume dilatation. Such dilatation is equal to the decrease in viscosity of localized shear bands of the glass.[10,27,28] When the fracture takes place, the local dilatation is larger enough to significantly lower the viscosity of the local shear bands, as if the local metallic glass is nearly melted. Figure 9(c) also shows the local melting features on the fracture surface. Such localized melting phenomena is evidentially observed during tensile and compressive testing experiments, and is also inspected by other investigators[12] in Zr-base BMGs.

The Zr-base BMG with quenched-in crystallites about 3 ~ 5% in volume fraction presents a typical brittle feature resulting in their tensile and compressive fracture strength lower

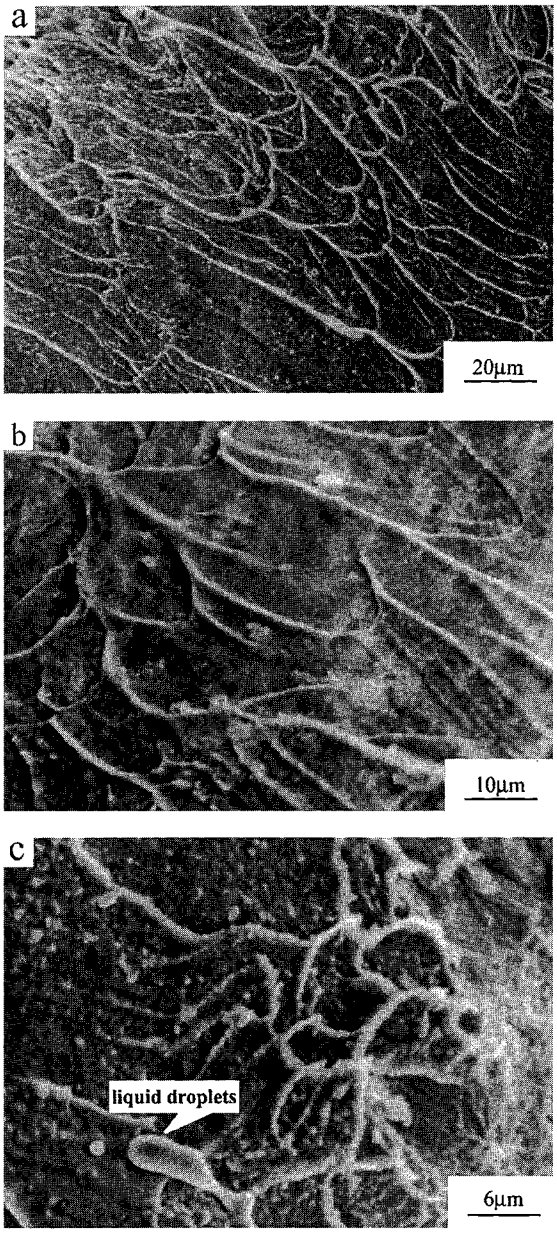

Fig. 9 SEM images of vein patterns (a and b) and liquid droplets on the fracture surface of $Zr_{52.5}Ni_{14.6}Al_{10}Cu_{17.9}Ti_5$ BMG.

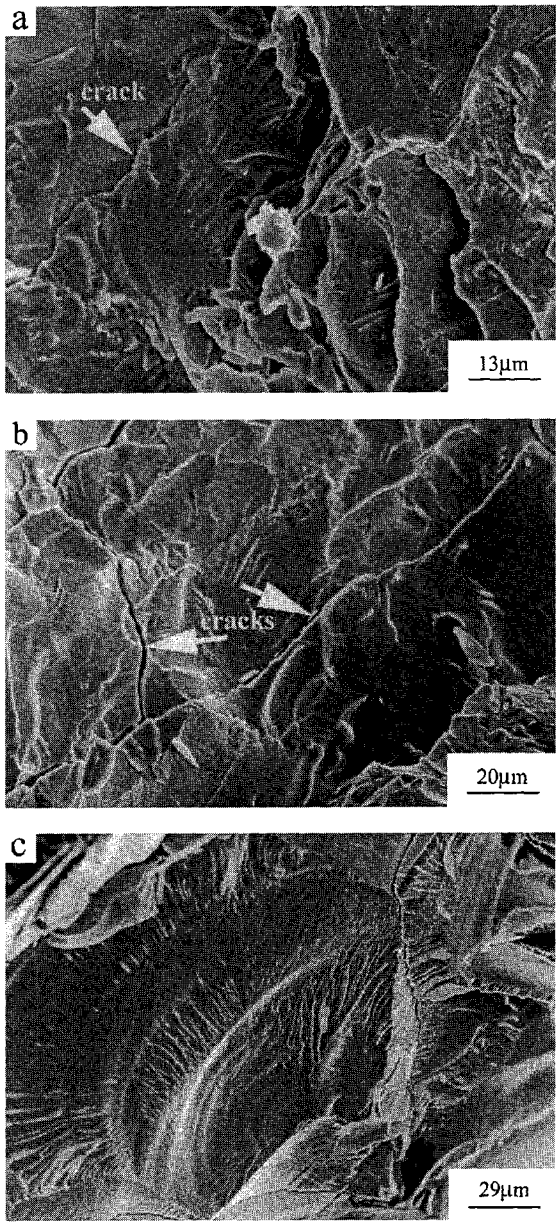

Fig. 10 Fracture features of $Zr_{52.5}Ni_{14.6}Al_{10}Cu_{17.9}Ti_5$ BMG with quenched-in crystallites of about 3 ~ 5% in volume fraction.

than that of the fully glass. The fracture surface becomes ambiguous compared with the fully glass. However, some ductile features, such as localized veins with obviously dilatation and local melting, can be observed on the brittle fractures. The quenched-in crystallites have played a significant role in the fracture strength and fracture modes, because they may initiate cracks in the interface between the crystallites and glass matrix due to the different mechanical properties, or, the weak interface can joint and speed up the crack propagation. Figures 10(a) and (b) show brittle cracks propagating in the specimen. Figure 10(c) represents the fracture surface on which a large size quenched-in crystallite is dropped from the glass matrix, which has contributed to the crack propagation and the occurrence of the fracture.

Figure 11 shows the typical brittle fracture features of the Zr-base BMG with quenched-in crystallites more than 5% in volume fraction. The high contents of crystallites in glass matrix dramatically decrease the tensile and compressive fracture strength. The fracture process apparently demonstrates brittle fracture manner. The corresponding fracture surface looks like rock strata between which there are many cracks as shown in Fig. 11. This kind of the microstructure makes the BMGs almost lose their strength. No any deformation strains before fracture can be detected.

4. Discussion

Even though the tensile and compressive stress-strain curves of the Zr-base BMG display no appreciable macroscopic plastic deformation before fracture, the fracture surface reveals typical ductile fracture manner, such as viscose flow traces, *i.e.* vein-like pattern morphology, and localized melting. The surface of the tensile and compressive specimens generates shear bands with typical orientations. The

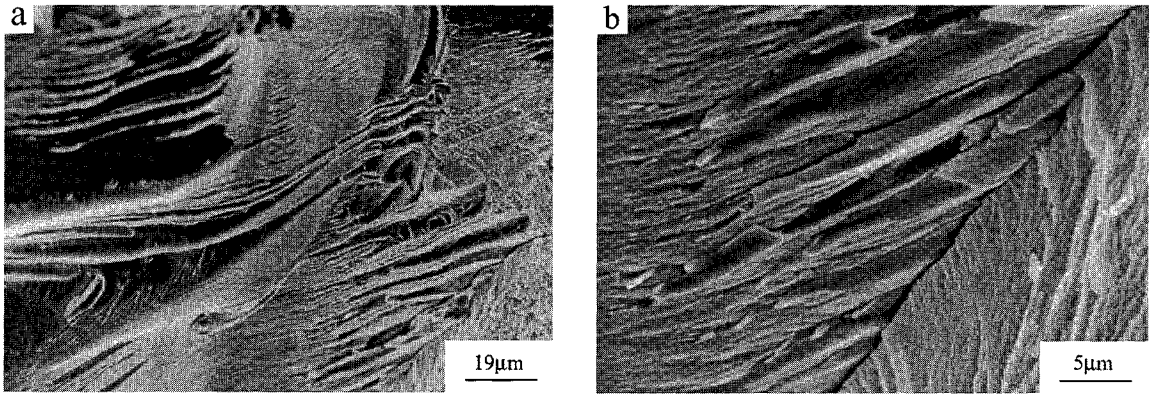

Fig. 11 Brittle fracture surfaces of $Zr_{52.5}Ni_{14.6}Al_{10}Cu_{17.9}Ti_5$ BMG with various volume fractions of crystalline precipitates.

formation mechanism of the shear bands had already suggested by Spaepen[10] and Argon.[28] The basic physical process underlying this inhomogeneous plastic deformation is a local softening of the glass. The localization of the flow in shear bands suggests that there is some structural change of the glass inside the bands. The structural change makes the plastic flow much faster in bands than in the rest of the specimen. This means that the shear band consists of a layer of the glass with lower yielding strength or lower viscosity than that of the rest of the specimen. Such weak layer is the potential fracture plane.

The softening of the glass in the shear bands is due to the structural change that accompanies a dilatation. Polk *et al.*[29] proposed that this structural change is the net result of two competing processes: shear-induced disordering and diffusion controlled reordering process. The inhomogeneous flow deformation of the BMGs is subjected to the condition of low temperature and high stress level. The shear-induced disordering during shearing of the glass is dominant. Its microscopic mechanism can be described as: an atom with hard-sphere volume V_{atom} can be squeezed into a neighboring hole with a smaller volume V_{hole} ($V_{hole} < V_{atom}$). This makes the neighbors of the new position move out, and creates a certain amount of free volume. The free volume in the shear bands is an important structural parameter, which governs the viscosity of the glass in the bands. An increase in free volume means the dilatation of the glass or the lowering of the viscosity in the shear bands.

In the view of thermodynamics, the dilatation corresponds to an increase in temperature. The increase in temperature in the local band on which fracture will occur has been evidently confirmed by finding of the liquid droplets on the fracture surface as clearly shown in Fig. 9(c). Liu *et al.*[12] had found the same local melting phenomena in the Zr-base BMGs. Bruck *et al.*[30] even detected an increase in temperature of higher than 500 centigrade in the shear band region in Be-bearing Zr-base BMG when conducting dynamic compressive tests at room temperature. As suggested by Liu *et al.*,[12] the local increase in temperature can be estimated from considering the conversion of the stored elastic strain energy to the adiabatic heating of a localized region at the moment of tensile or compressive fracture. Using this method, we can calculate the increase in temperature in the fracture shear band region to be 1028 K for compression and 1054 K for tension. They are

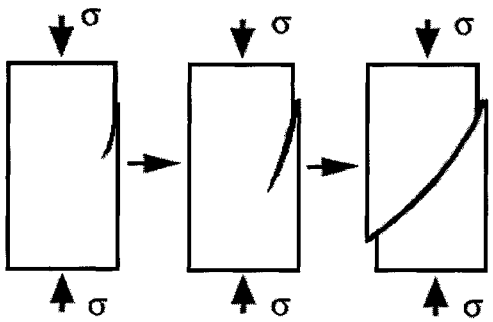

Fig. 12 Illustration of the shearing-off process and fracture of $Zr_{52.5}Ni_{14.6}Al_{10}Cu_{17.9}Ti_5$ BMG under compressive loading.

very near the melting point (1069 K[31]) of this Zr-base alloy. Such high temperature results in softening of the alloy in the fracture shear band region, which means that the viscosity of the alloy in the region would be as low as in 10^2 Pascal.[32,33] The lower viscosity is beneficial for shear flow; meanwhile, the shear flow deformation adds the strain energy and raises the local temperature. In this manner, once the shear bands approach their critical yielding stress, they will catastrophically fracture.

In the view of the phenomenology, the shearing-off takes place originally starting from the edge of the specimen, such as starting from a void or an edge crack that may be produced during the formation of the shear band. Once the shearing-off occurs, it will lead to the softening of the shearing-off bands. The softening bands then promote the development of the fracture crack. Furthermore, the crack propagates along the shear band orientation under the elevated loading till crossing whole body of the specimen. This fracture process is evidenced by Fig. 8 and is illustrated in Fig. 12. It is noticed that in the initial of the fracture, the fracture surface orientation is near the principal stress direction. With the development of the fracture crack, the fracture surface orientation rotates away from the principal stress direction to the maximum shear direction. Such rotation of the fracture surface is carried out by crossing the yielding shear bands as shown in Fig. 8. This suggests that the shear stress may play more important role in the fracture of the BMG under compression. With the yielding of the shear bands during the shearing-off process, each shear band leaves a flow trace behind on the fracture surface as shown in Fig. 7, and finally forms vein-like pattern fracture

morphology as shown in Fig. 9.

The difference of the fracture surface orientations between tension and compression suggests that the stress status in the specimen govern the formation of shear bands and fracture. The normal stress σ_n and shear stress τ_θ on a plane, which is away from the axis direction with an angle of θ, can be expressed as:

$$\sigma_n = \sigma_1 \sin^2 \theta \quad (1)$$

$$\tau_\theta = \sigma_1 \sin \theta \cos \theta \quad (2)$$

Where σ_1 is the principal stress, which is equal to the uniaxial tensile or compressive stress. In compression, the fracture occurs on the plane with $\theta = 45°$ on which the shear stress reaches its maximum, the normal stress is only half of its maximum and has the negative sign. The negative normal stress would impede the production of the free volume in the shearing-off bands. This suggests that the shear stress is the main controlling factor for the compressive fracture. In tension, however, the fracture occurs on the plane with $\theta = 56°$. On the fracture plane, the shear stress τ_{56} is about 93% of the maximum shear stress, and the normal stress is about 69% of the maximum normal stress (*i.e.*, principal stress) and has a positive sign. The positive normal stress certainly promotes the production of the free volume in the shearing-off bands. This suggests that the normal stress is also an important controlling factor for the tensile fracture. At $\theta = 56°$, the normal stress ($\sim 69\% \sigma_{n,max}$) and the shear stress ($\sim 93\% \tau_{max}$) reach equilibrium. Both govern the fracture process together.

When considering the strength, deformation and fracture modes of Zr-base BMGs with small volume fractions of quenched-in precipitates, we can simply take them as a metallic glass matrix/particulate composite for which the ductile glass matrix supplies toughness and ductility, and the crystalline precipitates contribute hardness. Under applied tensile or compressive stress, the cracks or deformation voids form in the ductile metallic glass containing crystalline precipitates either by precipitate fracture or by precipitate-matrix interface separation depending on the precipitate volume fraction, size, shape, and nature. Some micro-cracks or voids may already exist after the formation of the BMGs resulting from the residual stress around the precipitates due to the difference of the thermal expansion coefficients between the glass matrix and the predominant precipitates. They may initiate the fracture cracks or speed up the crack propagation in the presence of tensile or compressive loading. In addition, the existence of the crystalline precipitates may increase the elastic stress concentration in the glass matrix, *e.g.*, the maximum stress concentration on the boundaries of a near spherical precipitate is about 2.[24] For non-spherical precipitates, the stress concentration may reach much higher values. By the SEM and TEM observations, the crystalline precipitates in the Zr-base BMG have a near-spherical shape when their sizes are small. With increasing the precipitate sizes they will deviate from spherical shape and evolve to a hexagon even a triangle that will rise a higher stress concentration, resulting in cracking of the precipitates.

For avoiding the embrittlement of the Zr-base BMGs with quenched-in precipitates, we should control the volume fraction and maximum size of the precipitates. Hence, the addition of some elements, which can refine the quenched-in precipitate crystal size, should prevent the embrittlement. As we have known, the addition of Pd, Ag or Nb into Zr-base BMGs can cause the formation of finely crystals even nanocrystals which can keeps good ductility even for a large volume fraction of precipitates. In other respects, Ag, Pd, Au and Pt partially substitute Cu in Zr-base BMGs leading to the formation of a metastable quasicrystalline phase. Then the strength and ductility of the BMGs increase distinctly by the structural change upon precipitation of the nanoscale quasicrystals. However, the addition of those elements usually decrease the glass forming ability of the Zr-base BMGs.

5. Summary

The mechanical properties of $Zr_{52.5}Ni_{14.6}Al_{10}Cu_{17.9}Ti_5$ BMG were examined by tensile and compressive tests at room temperature. The fracture morphology of the BMG with quenched-in precipitates was comprehensively investigated by careful SEM observations. Following conclusions can be made:

(1) The compressive and tensile specimens were machined from $Zr_{52.5}Ni_{14.6}Al_{10}Cu_{17.9}Ti_5$ BMG casting rods and casting sheets, respectively. The compressive fracture strength of the Zr-base BMG is tested to be 1.82 ± 0.13 GPa corresponding to the total strain (including elastic and plastic strains) of 1.8%. The tensile fracture strength is 1.66 ± 0.42 GPa corresponding to the total strain of 1.6%.

(2) In tension, the fracture takes place along the shear band plane with about 56 deg from the axial direction. In the situation, both the normal stress, which is about 69% of the maximum normal stress, and the shear stress, which is about 93% of the maximum shear stress, reach a dynamic equilibrium and govern the fracture process together. In compression, however, the fracture occurs along the maximum shear stress plane with about 45° from the axial direction. The shear stress plays a more important role in the fracture process. Any shearing-off plane deviated from the maximum shear stress plane will rotates to the maximum shear stress plane under the elevated compressive loading.

(3) The fracture process of $Zr_{52.5}Ni_{14.6}Al_{10}Cu_{17.9}Ti_5$ BMG can be described as that the specimen firstly produce shear bands which are uniformly arranged in the specimen with band spacing about $0.2 \sim 0.5\,\mu m$, and then a random region on the specimen surface initiates shearing-off and generates a main fracture crack. Such crack propagates along the shear band plane till crossing whole body of the specimen under the elevated loading. For the bulk glass, any shearing-off induces a dilatation and softening of the glass in the shearing-off bands. The softening of the glass then promotes the plastic deformation and finally leads to the catastrophic fracture.

(4) On the fracture surface of $Zr_{52.5}Ni_{14.6}Al_{10}Cu_{17.9}Ti_5$ BMG, vein-like pattern is the typical morphology that is similar with that observed in other metallic glasses. It has demonstrated a well-known mechanism of fracture by the Taylor instability. The plastic deformation of the Zr-base BMG has a typical viscous flow feature.

(5) Local melting is another feature of the deformation and fracture of the Zr-base BMG. 'Liquid droplets' can be observed on the fracture surface. The increase in temperature

in the shearing-off region is due to the concentrated elastic strain energy transferring into thermal energy in the localized region. A thermodynamic calculation based on the conversion of the stored elastic strain energy to the adiabatic heating of the shearing-off region indicates the increase in temperature in the local region reaching more than 1000 K, which is very near the melting temperature of the Zr-base BMG alloy.

(6) The crystalline precipitates significantly influence the tensile and compressive properties. With increase in the volumetric fractions and the sizes of the precipitates, both the tensile and compressive strength and fracture strains decrease. The fracture mode changes from ductile to brittle. Vein patterns, shear-bands and local melting can still be observed when the volume fractions of quenched-in precipitates less than $3 \sim 5\%$. When precipitates exceed 5% in volume fraction, fracture surface becomes rock strata-like feature, and samples lose almost their strength. The precipitates with larger sizes and no-spherical shapes may play a role in rising stress concentration, resulting in decreasing the fracture strength.

Acknowledgements

The supports of China National High Technology Project (No. 863-715-005-0130) and Beijing Natural Science Foundation (No. 2992010) are gratefully acknowledged.

REFERENCES

1) A. Inoue: Acta Mater. **48** (2000) 279.
2) W. L. Johnson: Materials Science Forum **225–227** (1996) 35.
3) A. L. Greer: Science **267** (1995) 1947.
4) R. Doglione, S. Spriano and L. Battezzati: NanoStructured Materials **8** (1997) 447.
5) C. J. Gilbert, R. O. Ritchie and W. L. Johnson: Appl. Phys. Lett. **71** (1997) 476.
6) L. Q. Xing, C. Bertrand, J. P. Dallas and M. Cornet: Mater. Sci. Eng. **A241** (1998) 216.
7) A. Leonhard, L. Q. Xing, M. Heilmaier, A. Gebert, J. Eckert and L. Schultz: NanoStructured Materials **10** (1998) 805.
8) T. Zhang and A. Inoue: Mater. Trans., JIM **39** (1998) 1230.
9) F. Spaepen and D. Turnbull: Scripta Metall. **8** (1974) 563.
10) F. Spaepen: Acta Metall. **25** (1977) 407.
11) A. Inoue, T. Zhang and T. Masumoto: Mater. Trans., JIM **36** (1995) 391.
12) C. T. Liu, L. Heatherly, D. S. Eaton, C. A. Carmichael, J. H. Schneibel, C. H. Chen, J. L. Wright, M. H. Yoo, J. A. Horton and A. Inoue: Metall. Mater. Trans. **29A** (1998) 1811.
13) H. A. Bruck, A. J. Roosakis and W. L. Johnson: J. Mater. Res. **11** (1996) 503.
14) H. Kato and A. Inoue: Mater. Trans., JIM **38** (1997) 793.
15) A. Inoue, T. Zhang and Y. H. Kim: Mater. Trans. JIM **38** (1997) 749.
16) C. C. Hays, C. P. Kim and W. L. Johnson: Phys. Rev. Lett. **84** (2000) 2901.
17) U. Köster, J. Meinhardt, S. Roos and H. Liebertz: Appl. Phys. Lett. **69** (1996) 179.
18) U. Köster, J. Meinhardt, S. Roos and R. Busch: Mater. Sci. Eng. **A226/228** (1997) 995.
19) L. Q. Xing, J. Eckert, W. Löser and L. Schultz: Appl. Phys. Lett. **73** (1998) 2110.
20) A. Inoue, T. Zhang, M. W. Chen, T. Sakurai, J. Saida and M. Matsushita: Appl. Phys. Lett. **76** (2000) 967.
21) C. J. Gilbert, V. Schroeder and R. O. Ritchie: Metall. Mater. Trans. **30A** (1999) 1739.
22) M. W. Chen, A. Inoue, C. Fan and T. Sakurai: Appl. Phys. Lett. **74** (1999) 2131.
23) Z. Bian, G. He and G. L. Chen: Rare Metal Materials and Engineering, in press.
24) L. J. Broutman: *Composite Materials, (Vol. 5, Fracture and Fatigue)* (Academic Press, Inc., New York, 1974) pp. 45–93.
25) G. He, Z. Bian and G. L. Chen: Mater. Sci. Eng. **A279** (2000) 238.
26) Z. Bian, G. He and G. L. Chen: Scripta Metall. **43** (2000) 1003.
27) P. S. Steif, F. Spaepen and J. W. Hutchinson: Acta Metall. **30** (1982) 447.
28) A. S. Argon: Acta Metall. **27** (1979) 47.
29) D. E. Polk and D. Turnbull: Acta Metall. **20** (1972) 493.
30) H. A. Bruck, T. Christman, A. J. Roosakis and W. L. Johnson: Scripta Metall. **30** (1994) 429.
31) X. H. Lin, W. L. Johnson, W. K. Rhim: Mater. Trans., JIM **38** (1997) 473.
32) G. He, Z. Bian and G. L. Chen: Trans. Nonferrous Metals Society of China **9** (1999) 273.
33) G. He, Z. Bian and G. L. Chen: J. Materials Science and Technology, in press.